Electronic properties of graphitic surfaces with adsorbed aromatic amino acids

C. Roman*, F. Ciontu* and B. Courtois*

*Tima Laboratory, Grenoble, France, cosmin.roman@imag.fr

ABSTRACT

The electronic properties of aromatic amino acids physisorbed on graphene are investigated in view of establishing if carbon nanotube transconductance sensors are suitable for detecting this class of chemical stimuli. Several conclusions are drawn concerning both the sensitivity and selectivity of amino acid nanotube sensors based on results presented in the first part of this paper, while a series of methods for simplifying a self-consistent Hamiltonian down to a model, enabling accurate conductance calculations for systems of considerable size will be introduced in the second part. A case study is presented on which the aforementioned methods yield a minimal yet highly accurate set of parameters.

Keywords: carbon nanotubes, aromatic amino acids, *ab initio*, order reduction, renormalization

1 INTRODUCTION

Carbon nanotube applications are promoted daily by an ongoing effort within the theoretical and experimental community. Apart next generation transistors there is an increasing interest in biosensing applications motivated by the outstanding structural, mechanical and electrical properties of carbon nanotubes.

Selective sensors capable of determining the amino acid composition of a protein could prove extremely useful in experimental and theoretical proteomics, since the composition profile alone is often enough to identify a protein [1] or even predict its secondary structure [2,3]. However, the requirements in terms of sensitivity and dynamic range rule out most of the potential sensing mechanisms.

Carbon nanotube based chemical sensors have been experimentally demonstrated for NO_2, NH_3 [4], H_2 [5] and O_2 [6]. In this paper we will focus on similar transconductance devices, for which we aim to build a theoretical framework enabling the computation of quantum conductance modifications of two terminal carbon nanotube sensors in response to chemical stimuli, in the form of surface physisorbed amino acids. The discussions will be limited to zwitterion aromatic Histidine (HIS), Phenylalanine (PHE), Tryptophan (TRP) and Tyrosine (TYR) amino acids, binding through π stacking onto large radii carbon nanotubes.

The remainder of this paper is structured as follows. Section 2 is concerned with the *ab initio* calculations of systems involving graphene sheets and aromatic amino acids. The third section lays the theoretical grounds for our Hamiltonian order reduction procedure together with a renormalization algorithm designed to cancel eventual errors caused by the former procedure. A few conclusions are presented in the last section.

2 ELECTRONIC PROPERTIES

Simulating a sensor setup at a realistic, atomic level of detail is a formidable task. Moreover, when assessing the influence of parameters like the tube's radius and chirality, one cannot avoid using suitable approximations for the problem at hand. For example, re-computing the self-consistent Hamiltonian for each nanotube set of parameters is prohibitively expensive and vastly redundant, if the tube's radius is large. Curvature effects tend to vanish and the self-consistent Hamiltonian matrix elements of the flat graphene surface will provide a good approximation already.

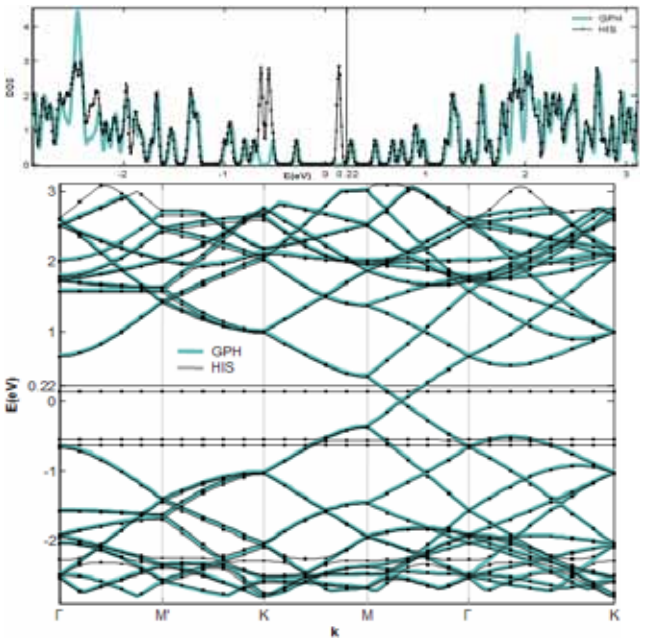

Figure 1: Total density of states and band structures for GPH+HIS. The cyan curves correspond to bare GPH.

A more detailed description of the *ab initio* calculations performed on these systems is contained elsewhere [7]. Here we focus only on those results considered relevant for the logic of our explanation.

Figure 1 displays the total density of states (TDOS) and band structure as obtained with SIESTA [8], in which the reference, pristine graphene (GPH) properties are plotted together with the same properties but for the GPH+HIS system. Typically the physisorption causes a 0.2 eV shift in the Fermi energy level, and introduces dispersionless bands close to E_f, whose positions depend on the amino acid, even though they were all found to be initiated by the $(COO)^-$ group. The existence of physisorption induced states close to E_f is considered a necessary condition for carbon nanotubes to be susceptible of detecting aromatic zwitterion amino acids.

Another result of Reference 7 emphasizes the strong localization of the charge perturbation around the $(COO)^-$ group. The spatial confinement of the perturbation establishes the validity of approximating amino acids on nanotube Hamiltonian matrix elements by their equivalents in a reference, amino acid on GPH system.

3 HAMILTONIAN MODEL REDUCTION AND RENORMALIZATION

This section deals with the formal tools we have developed for the task of reducing a self-consistent Hamiltonian in view of conductance calculation speed-up, while at the same time controlling the influence over numerical accuracy.

3.1 Elastic quantum transport formula

In this paper we consider only elastic transport within mean field theories like DFT, HF of TB, in which case Landauer-Büttiker like formulas are typically employed for computing the currents through molecular structures of the kind sketched in Figure 2.

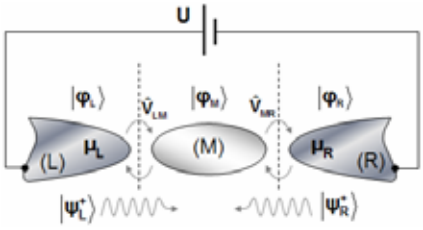

Figure 2: A generic electronic molecular device.

The following demonstrations rely on Todorov's derivation of the conductance, detailed in Reference 9, to which we refer the reader for a more thorough discussion. For consistency, here we repeat only a few expressions.

$$\hat{H} = \hat{H}_0 + \hat{V} = \left(\hat{H}_L + \hat{H}_M + \hat{H}_R\right) + \left(\hat{V}_{LM} + \hat{V}_{MR} + h.c.\right) \tag{1}$$

The Hamiltonian of the system sketched in Figure 2 is decomposed in a sum of two terms; one describing the three distinct regions of the device ((L)eft lead, (M)olecular system and (R)ight lead), and the other describing the interactions between these regions (see Equation 1).

Denoting the Green's function of the system by $\hat{G}^r(E)$

$$\hat{G}^r(E) := \lim_{\varepsilon \to 0^+} \left[E - \hat{H} + i\varepsilon \right]^{-1} \tag{2}$$

and by $\hat{\rho}^0(E)$ and $\hat{t}(E)$

$$\hat{\rho}^0(E) := \delta(E - \hat{H}_0) \tag{3}$$

$$\hat{t}(E) := \hat{V} + \hat{V}\hat{G}^r(E)\hat{V} \tag{4}$$

Todorov's formula for the current's expectation value reads:

$$\left\langle \hat{I} \right\rangle = \frac{2\pi e}{\hbar} \int dE \, \mathrm{Tr}\left[\hat{\rho}_L^0(E)\hat{t}^\dagger(E)\hat{\rho}_R^0(E)\hat{t}(E) \right] \times \\ \times \left[f(E-\mu_R) - f(E-\mu_L) \right] \tag{5}$$

where $\hat{\rho}_n^0(E) = \hat{\rho}^0(E)\hat{P}_n$, $\hat{P}_n$ being the projection operator $\hat{P}_n = \sum |\varphi_n\rangle\langle\varphi_n|$ onto the free lead states, and *f(E)* being the Fermi-Dirac distribution. The trace is over all the states $\{|\varphi_n\rangle\}$ of the free Hamiltonian $\hat{H}_0$. After a few manipulations on Equation 5 one gets

$$\left\langle \hat{I} \right\rangle = \frac{2\pi e}{\hbar} \int dE \, \mathrm{Tr}\left[w^\dagger(\hat{H}_0)\hat{O}(E)w(\hat{H}_0) \right] \tag{6}$$

Here $\hat{O}(E)$ is just a compact notation of $\hat{\rho}_L^0(E)\hat{t}^\dagger(E)\hat{\rho}_R^0(E)\hat{t}(E)$ and $w(\hat{H}_0)$ a compact notation of $\left[f(\hat{H}_0 - \mu_R) - f(\hat{H}_0 - \mu_L) \right]^{1/2}$

The transformation of the Fermi-Dirac distribution into an operator was possible because of the following identity:

$$\hat{\rho}^0(E) f(E-\mu_n)|\varphi_n\rangle \equiv \hat{\rho}^0(E) f(\hat{H}_0 - \mu_n)|\varphi_n\rangle \tag{7}$$

Next, we have to rewrite Equation 6 in a non-orthogonal basis, since in most of the practical calculations the states $\{|\varphi_n\rangle\}$ are expanded into a linear combination of atomic like orbitals $\{|i\rangle\}$. By using the closure relation for non-orthogonal bases $\sum_{i,j} |i\rangle \mathbf{S}_{\mathbf{ij}}^{-1} \langle j| \equiv 1$ where $\mathbf{S}_{\mathbf{ij}} = \langle i|j\rangle$, Equation 6 transforms into

$$\left\langle \hat{I} \right\rangle = \frac{2\pi e}{\hbar} \int dE \, \mathrm{Tr}\left[\mathbf{S}^{-1/2}\mathbf{w}(\hat{H}_0)\mathbf{S}^{-1}\mathbf{O}(E)\mathbf{S}^{-1}\mathbf{w}(\hat{H}_0)\mathbf{S}^{-1/2} \right] \tag{8}$$

Computing the matrix elements of $w(\hat{H}_0)$ in a non-orthogonal basis is somehow tricky. We have derived a numerically stable formula for computing this matrix

$$\mathbf{w}(\hat{H}_0) = \mathbf{H_0}\mathbf{S}^{-1/2} w_{\perp}(\mathbf{S}^{-1/2}\mathbf{H_0}\mathbf{S}^{-1/2})\mathbf{S}^{1/2}\mathbf{H_0}\mathbf{S} \quad (9)$$

where $w_{\perp}(\mathbf{X})$ means the function of the **X** matrix supposedly written in an orthogonal basis, and thus computable in terms of **X**'s eigenvector matrix **V** and eigenvalues diagonal matrix **D**, using the classical formula $\mathbf{V}w(\mathbf{D})\mathbf{V}^{\dagger}$.

At this point we wish to make a key observation. Equation 8 would have been nothing more than a transcription of Todorov's formula if it were not for the special structure of the $\mathbf{S}^{-1/2}\mathbf{w}(\hat{H}_0)\mathbf{S}^{-1}$ matrix and its hermitean conjugate $\mathbf{S}^{-1}\mathbf{w}(\hat{H}_0)\mathbf{S}^{-1/2}$ which frame $\mathbf{O}(E)$.

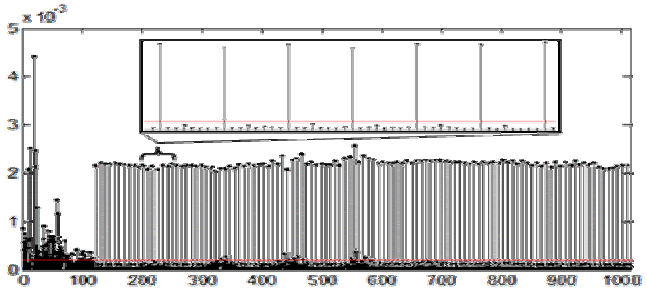

Figure 3: Column average of HIS - $\mathbf{S}^{-1}\mathbf{w}(\hat{H}_0)\mathbf{S}^{-1/2}$ matrix.

Figure 3 has the purpose of emphasizing the special structure of $\mathbf{S}^{-1/2}\mathbf{w}(\hat{H}_0)\mathbf{S}^{-1}$ matrix. It represents the average of the absolute values of this matrix along its columns. As it can be observed, only a few of its columns are populated and these ones will select only corresponding lines of $\mathbf{O}(E)$. Here, selecting means that, since entire columns of $\mathbf{S}^{-1/2}\mathbf{w}(\hat{H}_0)\mathbf{S}^{-1}$ are almost zero, it doesn't matter what are the values of the corresponding lines in $\mathbf{O}(E)$. The same is true for $\mathbf{S}^{-1}\mathbf{w}(\hat{H}_0)\mathbf{S}^{-1/2}$ but in terms of the columns of $\mathbf{O}(E)$. Based on these observations we can ignore all together many of the lines and (corresponding) columns of $\mathbf{O}(E)$ operator without affecting the current's expectation value. This operation is equivalent to eliminating atomic orbitals of the basis, and working in a subspace of the original Hilbert space. Naturally this sub-space projection has a significant influence over computation time and is one of the main results of our work.

3.2 Isospectral matrix flows

The sub-space projection method described in the previous section has, to no surprise, at least one problem in practice. The elimination of atomic orbitals from the basis set perturbs, depending on the system under study, the band structures, as can be observed for instance in Figure 4 top-left.

A second problem, which has more to do with the limited size of the GPH super cell than with the orbital elimination procedure, made us consider renormalizing the Hamiltonian and overlap matrices (**H**, **S**), i.e. modifying their elements so as to simultaneously satisfy given spectral and structural constraints.

Our renormalization procedure is an adaptation of Chu's least squares approximation of symmetric-definite pencils subject to generalized spectral constraints [10] to which we refer the reader for a rigorous introduction to the mathematical concepts. In simple terms the procedure consists in finding a pair of matrices (**H**, **S**) that yield the same eigenvalues as some pair ($\mathbf{H}_0$, $\mathbf{S}_0$) and are as close as possible, element-wise, to some other pair ($\mathbf{H}_{\perp}$, $\mathbf{S}_{\perp}$).

As the set:

$$\mathcal{M}(\mathbf{H}_0, \mathbf{S}_0) := \left\{ \left(\mathbf{T}\mathbf{H}_0\mathbf{T}^{\mathbf{t}}, \mathbf{T}\mathbf{S}_0\mathbf{T}^{\mathbf{t}} \right) \in \mathbb{R}^{n\times n} \times \mathbb{R}^{n\times n} / \det(\mathbf{T}) \neq 0 \right\}$$

consists of *all* symmetric definite pairs having the same eigenvalues with ($\mathbf{H}_0$, $\mathbf{S}_0$), the problem reduces to finding a congruence transformation matrix **T** such that (**H**, **S**) ≡ ($\mathbf{T}\mathbf{H}_0\mathbf{T}^{\mathbf{t}}$, $\mathbf{T}\mathbf{S}_0\mathbf{T}^{\mathbf{t}}$) optimally approximates ($\mathbf{H}_{\perp}$, $\mathbf{S}_{\perp}$). Formally, this is equivalent to finding the minimum of the following expression:

$$F(\mathbf{T}) := \frac{1}{2}\left(\left\| \mathbf{W_H} \circ (\mathbf{H} - \mathbf{H}_{\perp}) \right\|_F^2 + \left\| \mathbf{W_S} \circ (\mathbf{S} - \mathbf{S}_{\perp}) \right\|_F^2 \right) \quad (10)$$

where $\circ$ is the Hadamard matrix product and $\|\mathbf{X}\|_F^2$ the Frobenius matrix norm. The two weighting matrices ($\mathbf{W_H}$, $\mathbf{W_S}$) represent the only distinction between our renormalization procedure and Chu's theory [10]. They allow in a straightforward manner to increase, decrease or even cancel any individual matrix element of **H** or **S**.

One major feature of isospectral flows is that the gradient of $F(\mathbf{T})$ is analytically computable; in our case

$$\nabla F(\mathbf{T}) = 2\left(\left[(\mathbf{W_H})_{\circ}^2 \circ (\mathbf{H} - \mathbf{H}_{\perp}) \right] \mathbf{T}\mathbf{H_0} + \left[(\mathbf{W_S})_{\circ}^2 \circ (\mathbf{S} - \mathbf{S}_{\perp}) \right] \mathbf{T}\mathbf{S_0} \right) \quad (11)$$

which makes it possible to quickly set-up a steepest descent flow in order to find the minimizer of Equation 10, i.e. the solution to our problem.

$$\dot{\mathbf{T}}(t) := -\nabla F(\mathbf{T}(t)) \quad (12)$$

We have applied this method to GPH+HIS system, whose properties before the renormalization process are found in the left column of Figure 4, where the two problems mentioned at the beginning of this sub-section are clearly visible; some bands are perturbed and the charge redistribution following physisorption extends throughout the unit cell. Due to the renormalization procedure's flexibility we were able to address simultaneously the two, apparently different, problems.

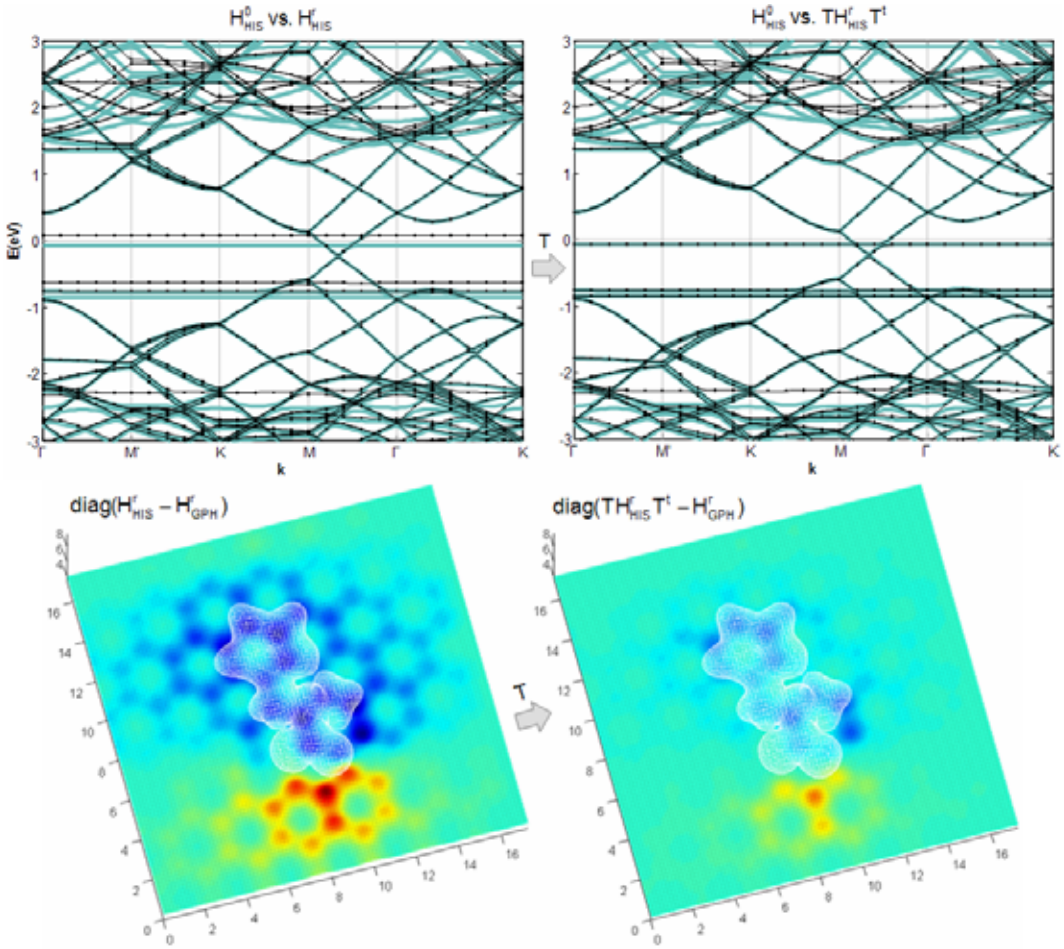

Figure 4: (Top) HIS band structure after orbital elimination (left) and after renormalization (right). (Bottom) Diagonal Hamiltonian elements represented in real space before (left) and after renormalization (right)

If $\mathbf{H}^r\mathbf{\Psi} = \mathbf{S}^r\mathbf{\Psi E}$, correcting the spectrum of the reduced system is simply a matter of replacing the eigenvalues diagonal matrix **E**. Thus $\mathbf{S}_0 = \mathbf{S}^r$ and $\mathbf{H}_0\mathbf{\Psi} = \mathbf{S}_0\mathbf{\Psi E}_0$ with $\mathbf{E}_0$ the exact spectrum.

Through this transformation the sparsity of the initial ($\mathbf{H}^r$, $\mathbf{S}^r$) is lost but fortunately by properly choosing the matrices ($\mathbf{W}_H$, $\mathbf{W}_S$) within the isospectral flow we were able to recover the sparsity, conserve the spectrum and even confine the physisorption charge perturbation into a smaller region of the unit cell as visible in Figure 4 bottom.

4 CONCLUSIONS

In this paper we have proposed a novel bottom-up approach for Hamiltonian order reduction in view of speeding-up quantum conductance calculations. In a first phase, vectors from the initial basis are eliminated if found not to contribute to the trace appearing in Equation 8. Eventual errors introduced in the first phase are corrected through a renormalizing isospectral flow. The result is a matrix pair (**H**, **S**) of unprecedented accuracy-to-rank ratio.

REFERENCES

[1] Wilkins M.R. *et al.*, *Biochem. Biophys. Res. Commun.* **221**, 609 (1996)

[2] Eisenhaber F., Imperiale F., Argos P., Froemmel C., *Proteins: Struct., Funct., Design* **25**, 157 (1996) N2

[3] Eisenhaber F., Froemmel C., Argos P., *Proteins: Struct., Funct., Design* **25**, 169 (1996) N2

[4] J. Kong *et al*., *Science* **287**, 622 (2000)

[5] J. Kong, M. G. Chapline, H. Dai., *Adv. Mater.* **13**, 1384 (2001)

[6] P. G. Collins, K. Bradley, M. Ishigami, A. Zettl., *Science* **286**, 1801 (2000)

[7] C. Roman, F.Ciontu, B. Courtois, *Proceedings of EMN04* (2004)

[8] J. M. Soler *et al.*, *J. Phys.: Condensed Matter* **14**, 2745 (2002)

[9] T. N. Todorov, G. A. D. Briggs, A. P. Sutton, *J. Phys.: Condensed Matter* **5**, 2389 (1993)

[10] M.T. Chu and Q. Guo, *SIAM J. Matrix Anal. Appl.* **19**, 1 (1998)